# Gold and Antimony Mineralizations of Jbel Haouanite (High Atlas, Morocco) in Their Geodynamic Context

***Azza Addi, PhD***
***Boushaba Abdellah, PES***
***Moukadiri Ali, PES***
Université Sidi Mohamed Ben Abdellah, Laboratoire LISTA,
Faculté des Sciences, Atlas-Fès, Maroc

Doi: 10.19044/esj.2019.v15n18p336 URL:http://dx.doi.org/10.19044/esj.2019.v15n18p336

**Abstract**

The gold and antimony mineralizations of Jbel Haouanite (Eastern High Atlas, Morocco) are hosted by quartz veins in tectonic structures carried by Ordovico-Silurian Paleozoic formations. At least three phases of folding tectonics affected the area, inducing three generations of folds accompanied by two flow schistosities and a fracture one. Magmatic intrusions of a rhyodacitic nature are post-Silurian and prior to mineralization. From a mineralogical point of view, paragenesis includes native gold, stibnite, valentinite, stibiconite, as well as antimony and lead sulfosalts. Petrographic studies and chemical analyzes show the lack of correlation between gold and the different elements. Thus, the gold would have deposited later to antimony and is associated with oxidation minerals, especially valentinite. The results of the analyzes on different diagrams makes it possible to conclude that the gold mineralizations are of the mesozonal to epizonal orogenic type and they would be late-Hercynian.

**Keywords:** Meso-epizonal Gold, Antimony, Folding Tectonics, Jbel Haouanite, Morocco

## Introduction

The Tamlalt Plain is a buttonhole of the eastern Moroccan Meseta where Precambrian and Paleozoic lands outcrop between the Mesozoic and Cenozoic formations of the Eastern High Atlas (Fig. 1). This region is particularly famous for the mineralization of barite of Jbel Zelmou and for the galena and the manganese of Bouarfa. However, a growing interest is starting to be given to the gold and antimony mineralizations at Jbel Haouanite (aim of this work) and gold and copper from Jbel Menhouhou (south of the

buttonhole). Indeed, while the exploitation of galena and manganese are quite old, the discovery of gold in the Tamlalt dates back to the beginning of the 70s of the last century but its exploitation was undertaken only towards the end of the century.

The gold and antimony mineralizations of Jbel Haouanite are located in the northern zone of the plain, at the piedmont of the northern Atlas Ridge, about 70 km west of Bouarfa. Access to the site is via a track of about thirty kilometers at Mengoub to Atchana on the road from Bouarfa to Errachidia.

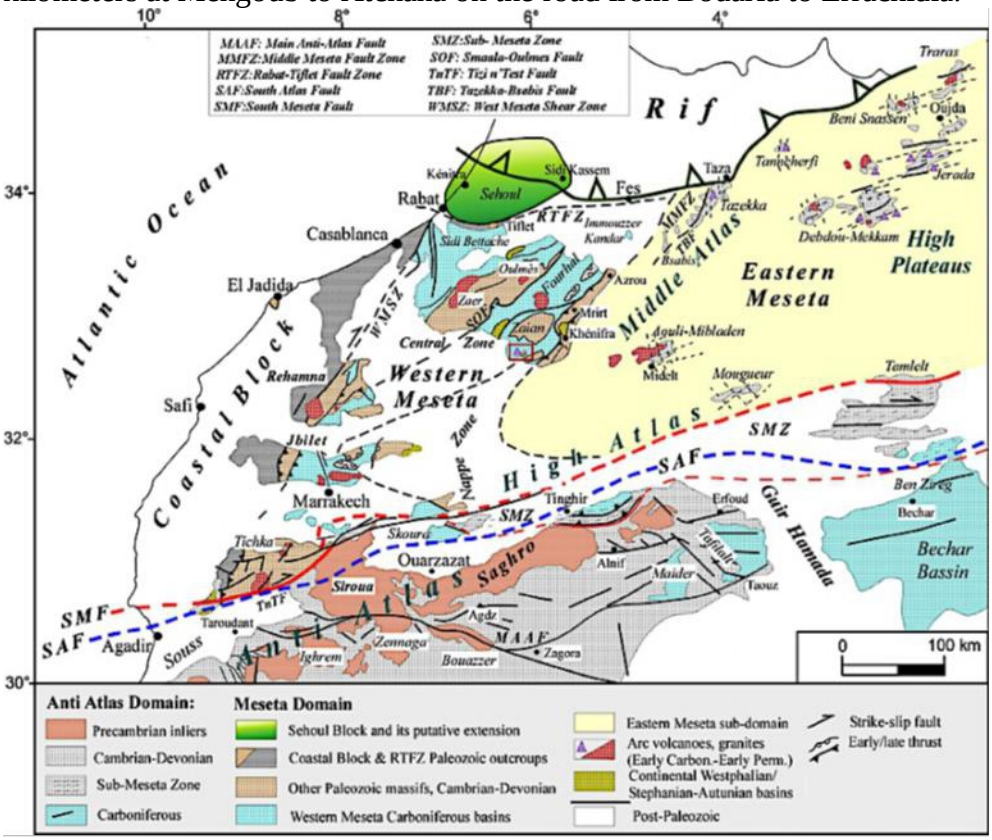


**Figure 1:** location of the studied area (blue rectangle) on the simplified structural map of the Moroccan Meseta and the NW part of the Anti Atlas (Hoepffner et al., 2005).

## Materials and methods

For the characterization of the mineralogical composition of mineral species, we proceeded on the one hand to the study by (i) "X'Pert" diffractometry, the results of which were interpreted using "Highscore" analysis software; then by (ii) QEMSCAN (Quantitative Evaluation of Minerals by SCANning electron microscope) based on Johannesburg SGS standards, and finally by (iii) scanning electron microscopy (SEM) and light microscopy. In addition, we carried out an ICP analysis of 37 samples of all

types combined (Table 1, in annex), at the Laboratory of the National Office of Hydrocarbons and Mines in Rabat (ONHYM).

## Results and discussion

### Stratigraphy

The first geological cross section was established by Rey in 1911 where he defined the Silurian formations by Graptoliths. Subsequent studies have identified other formations including Proterozoic, particularly in the south of the Plain and Paleozoic in the Center.

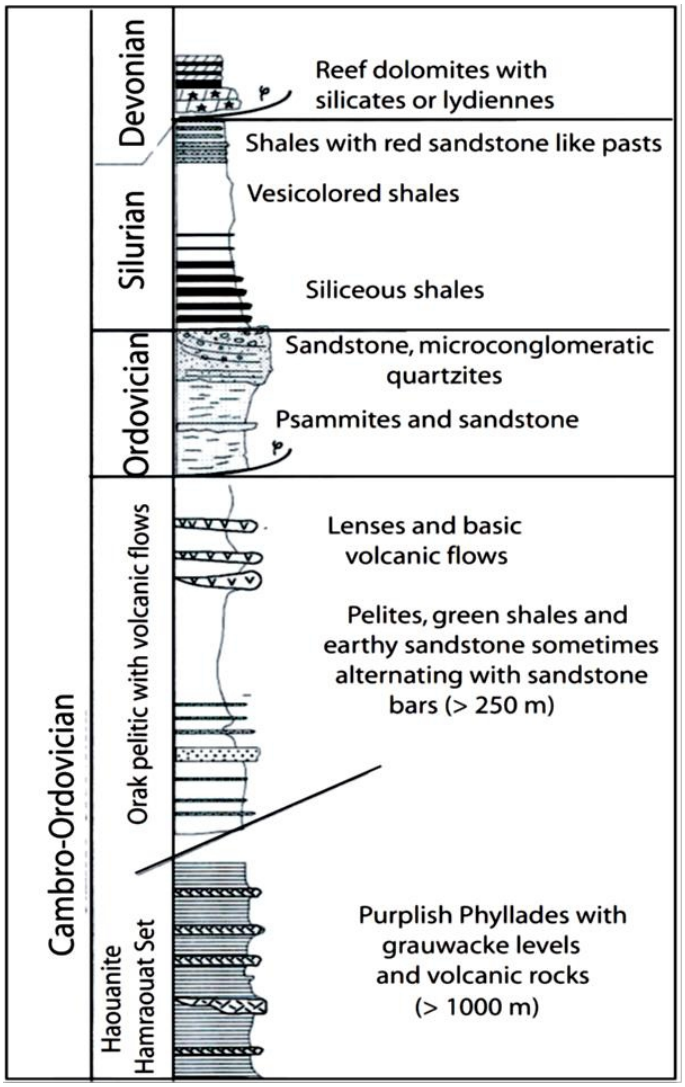


**Figure 2:** Synthetic lithostratigraphic column of the plain of Tamlalet (Houari, 2003, modified).

Mesozoic points (mainly Lower Jurassic) complete the entire plain mainly with quaternary cover. Figure 2 presents a schematic stratigraphic column indicating a comparison between the northern domain (area of our study) and the central-southern area.

The Proterozoic of the southern part (JbelTioua) would include according to Choubert et al. (1950), an inferior formation, called "lower volcano-detritic formation", with rhyolites, shales, conglomerates as well as sandstones and limestone blocks; a median formation with calcareous ferruginous concretions and a superior formation with limestones, in benchs and bodies, often lenticular. These sets are separated from the Infracambrian by a ferruginous hardground marking the end of a serie of metatuffites and metacinerites. The boundary between Proterozoic and Paleozoic is marked by an infracambrian calcareo-dolomitic formation ranging in thickness from 70 to 250 m (Pelleter 2007, Pelleter et al. 2008).

The Cambro-Ordovician grouped all the schisto-quartzitic formations located under the Silurian graptolite formations. These lands are outcropping along the southern edge of the northern border chain and in the Jbel Haouanite region, Ain Lorak, as well as in the southern part of the buttonhole, where they have been described particularly by Bolata (1995) and Khoukhi (2002). Structural analyzes and facies similarity approaches, however, made it possible to distinguish between Cambrian and Ordovician formations. This is how Milhi et al. (2010) attribute the "Cambro-Ordovician" formations from the northern part of the plain to the lower to medium Cambrian, similar in facies to the lands described by El Kochri (1981) in the Mouguer buttonhole. For Khoukhi (2002), the serie is made up of greenish satinised quartzo-phyllites, with grauwackes and interbedded volcano-sedimentary material. For Pelleter (2007), the base of Paleozoic is composed of black or green pelites, more or less sandstone like and whose power can reach 800m. These formations were dated by Trilobites and attributed to the Middle Cambrian. The Ordovician would include sandstone, shales, clays and quartzitic beds and ends with micro-conglomerates.

The Silurian rests above the "Cambro-Ordovician" formations and is dated by the Graptolites (Dresnay and Wilfert, 1960).

According to Houari (2003), the serie comprises, at the base, shales in platelets with siliceous lenses in the form of black and gray phtanites on which silty versicolores shales are based and ending in schists with centimetric to decimetric intercalations of sandstones, quartzites and pelites.

The Devonian was described by Dresnay and Lafuste (1960) as outliers, of very small extension dolomitic brown-chocolate limestone, organized in decimetric to metric benches often verticalized with black lydian stones (2-5 cm) indicating the stratification. The outcrops are taken up in a corridor of posterior faults N70 to N80 and show neither fold nor schistosity.

**Magmatism**

According to Milhi et al. (2010), several Hercynian and Triassic veins and dykes (microgranites, microgabbros, diabases) intrude the serie. The microgranites are slightly altered and composed of quartz, potassium feldspar (orthoclase) and microcline. The green rocks, quite altered, are formed of microgabbros and diabases. They have a crystallized microlithic bottom with minerals of epidote, plagioclase, pyroxene (augite) and pyrite. Amphibolite dykes are scarce.

During field surveys, we noted the presence of several blades of magmatic rocks very often associated with tectonic slaces. The petrographic study allowed us to distinguish two generations of magmatism, one of which is post-Silurian since it induced a contact metamorphism, with spotted andalusite shale; but this intrusion remains anterior to the second phase of folding in view of the schistosity it collects.

Regarding the first generation, it is a clear rock, microgranular, very altered. The petrographic study shows a rock with a clear schistosity, dominant quartz and plagioclase, altered (argilitization) and corroded. Biotite is stretched, oriented and altered. Mesostasis is composed of micas (muscovite, chlorite) and quartz. Some quartz grains are rounded, reflecting the hot conditions of the crash. Other minerals include garnet and apatite.

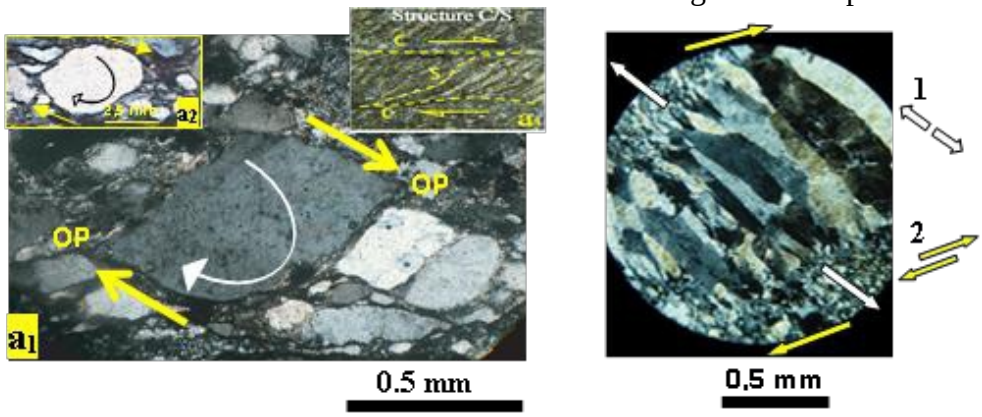


**Figure 3:** crystals of dextral sheared granite quartz (a1 and a2) and shist micas (a2) associated with recrystallization of quartz veins in elongated quartz fibers in the direction of opening (b) perpendicular to dextral shear . OP: Shadow of Pressure, 1: Direction of recrystallization of quartz (stretching), 2: Shear direction

Similarly, feldspar ghosts completely altered in micas (clays, sericite, etc.) are observed with oxides and crystals of rolled quartz, oriented and showig pressure shadows (Fig. 3). And, as described by Ingles et al. (1999), this form of crushing and stretching of quartz recrystallized in fiber in the opening directions characterizes a shear-zone.

Tourmaline and opaque minerals have been observed in the rock, reflecting the gneissic nature of the rock.

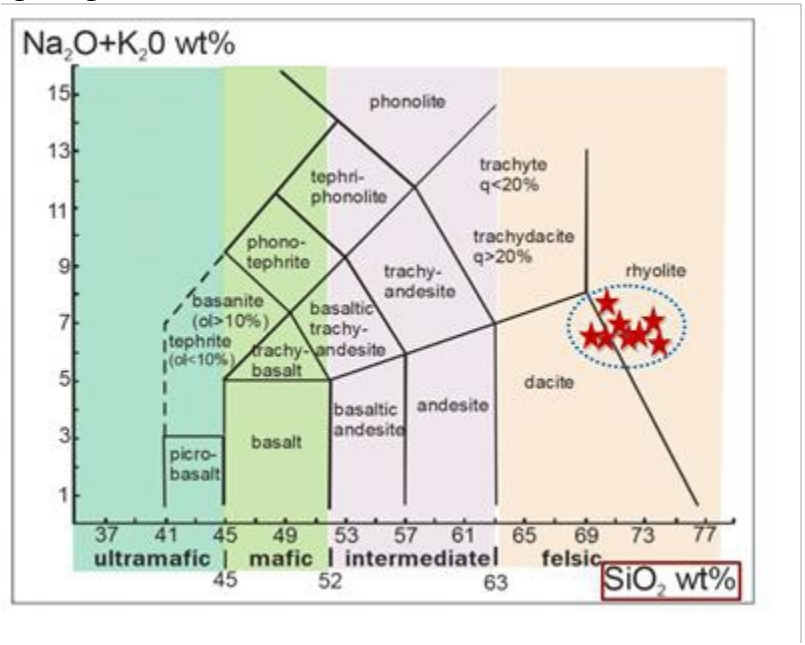


**Figure 4:** TAS diagram indicating the nature of Jbel Haouanite magmatic rocks

The presence of tourmaline (hence the Boron) leads that it is contemporary with the circulation of hydrothermal fluids. For the second generation, the chemical analyzes (table 4, in annex) make it possible to classify it as a rhyo-dacite, according to the TAS diagram (fig. 4).

**Tectonics**

The area has undergone a polyphase tectonic history. Concerning the brittle structures, and in addition to the flat faults observable in the galleries and the well, it is necessary to point out first the EW faults, often senestre, which, considering the streaks which one can observe locally, have had to be replayed several times (fig.5). With the N70 faults, they constitute the essential of the mineralized corridors. These directional structures (parallel to the atlasic chain) are chopped by N-S transverse faults which cut out mineralized panels (fig.6) showing a metallographic microscope association between gold and antimony oxides (fig.7).

To these main structures are associated N20-30 faults and N120-140 cracks. The analysis of this system is reminiscent of what has already been described in the Tafilalet (Azza and Makkoudi, 1996) with a sinistral detachment N70 following a maximum stress σ1 oriented N20-30.

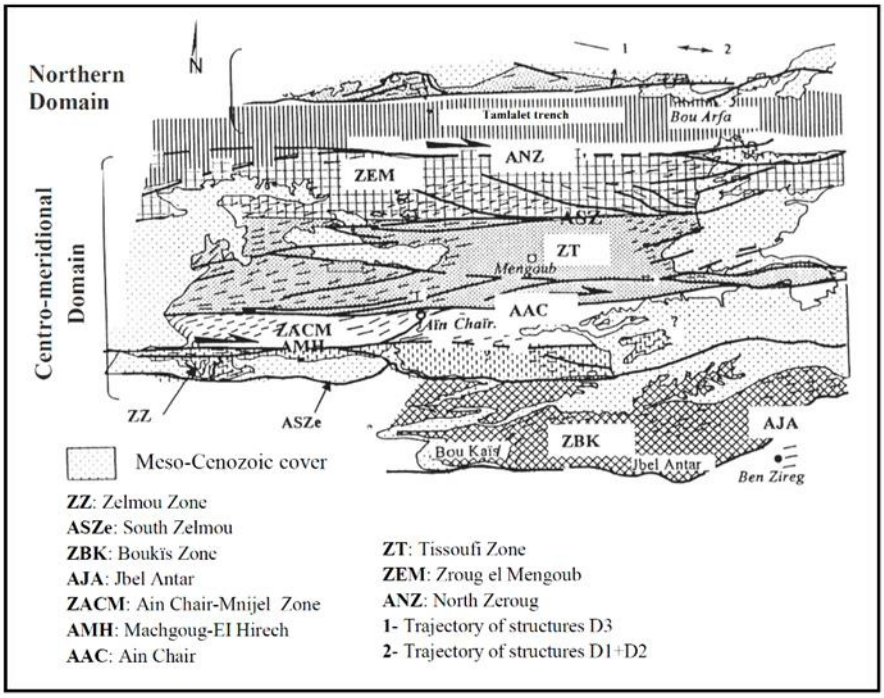


Figure 5: Structural map of the Tamlalt buttonhole (Houari and Hoepffner, 2003)

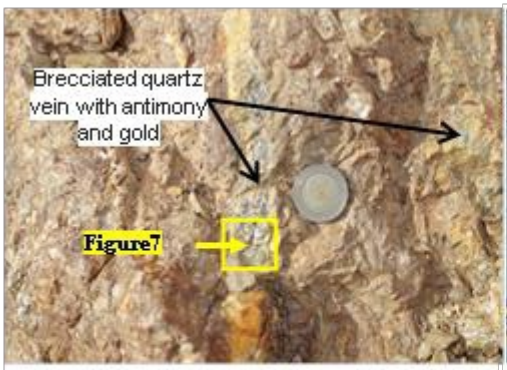


Figure 6: Antimony quartz vein and Gold in the shaly-host of the Jbel Haouanite deposit

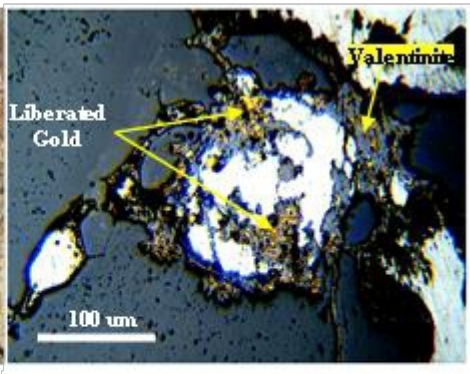


Figure 7: Metallographic microscope image showing the association between gold and antimony oxides from the Jbel Haouanite deposit

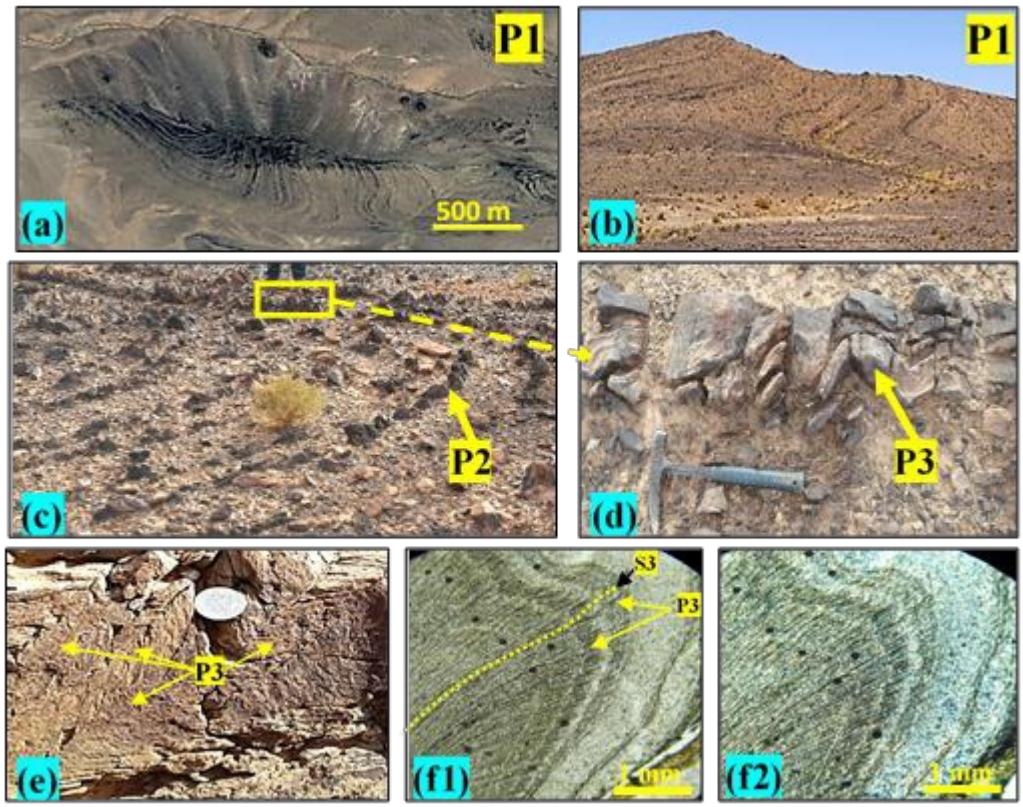


**Figure 8:** folds P1 seen by satellite (a) and panoramic view (b), P2 (c) and P3 (d) affecting the sandstone like schists. f1 f2 represent respectively a microscope view with natural light and polarized and analized light shales affected by schistosities S0-1, S2 and S3.

These events can be observed both in the field (Figs 8 a, b and c) and in the microscope (Fig 8 d). These results make it possible to refine the previous studies (Hoepffner, 1987, Boutib, 2000, Houari and Hoepffner, 2000) which allowed to define several phases of folding:

- A Breton phase with two episodes D1 and D2 affecting the Ain Lorak formation and inducing P1 and P2 folds with flow schistosities;
- A post-Westphalian phase D3 responsible for the different strike structures at the origin of the right to slightly dumped to the North P3 folds.

## Mineralizations

For the characterization of the mineralogical composition of the mineral species, we proceeded on the one hand to the study by X-ray diffractometry (Figs 9 a and b) and then to the analysis of certain samples by scanning electron microscopy (figs. 10a, b) and by infrared spectrometry (Figs 11a and b). Finally, the metallographic microscope study showed the presence

of native gold grains of micrometric size in the pure state, closely related to valentinite or very rarely free in gangue quartz (Figure 7).

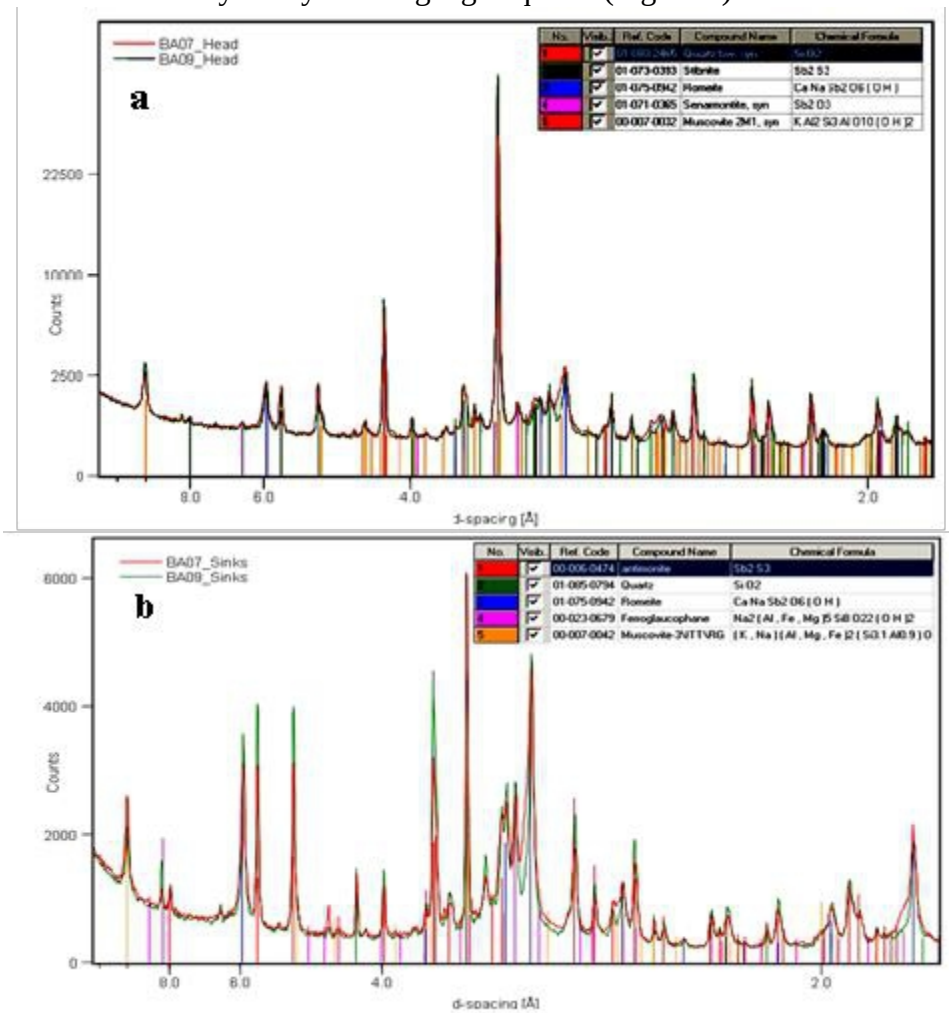


**Figures 9 a and b:** X-ray spectrum of the mineralizations of the Jbel Haouanite

X-ray diffraction analyzes revealed the presence of quartz, muscovite, calcite and an amphibole that may be glaucophane (Figs 9 a and b). Among the metallic minerals determined from their peaks in the diffractogram, stibnite (Sb2O3), roméite (CaNaSb2O6 (OH)), senarmontite (Sb2O3) and pyrrhotite in small quantities are reported.

Quantitatively, the sample composition is dominated by silicates (between 69 and 81%) with quartz (60 to 73%), muscovite (4.2 to 6.3%), plagioclase (1.7 to 2%), amphibole (1.1 to 1.3%) and traces of chlorite (<0.5%). On the other hand, the total content of sulphides is less (between 8.5 and 13%) with a predominance of stibnite (between 7.4 and 11.7%) but with

the presence of pyrrhotite (1 to 1.6%) as well as traces of galena (0.1%) and blende.

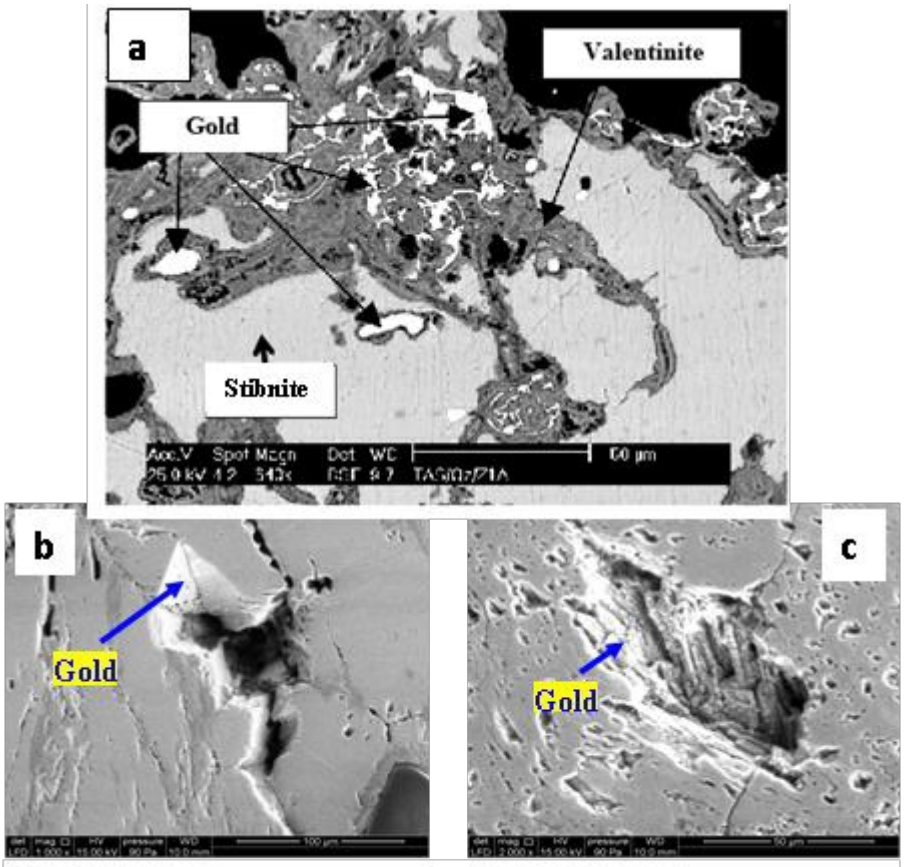


**Figure 10:** Scanning Electron Microscope images of the gold from the Haouanite deposit (a, b and c) (a is from Alansari, 2008).

To this, it is necessary to add oxides and hydroxides of antimony (5 to 9%) as well as carbonates including calcite (3.3 to 6.2%) and dolomite (1.2 to 1,7%).

This study confirms that gold is always free, either associated with antimony oxides (valentinite) or in fractures (Figs 6, 7 and 10 a-b). Let us recall that the study carried out by Vasquez Lopez (1974) made it possible to highlight stibnite, pyrite, gold in grains, bindheimite (Pb2Sb2O6 (O, OH)), native antimony and lead sulfosalts and valentinite, which serves as a research guide for prospecting workers.

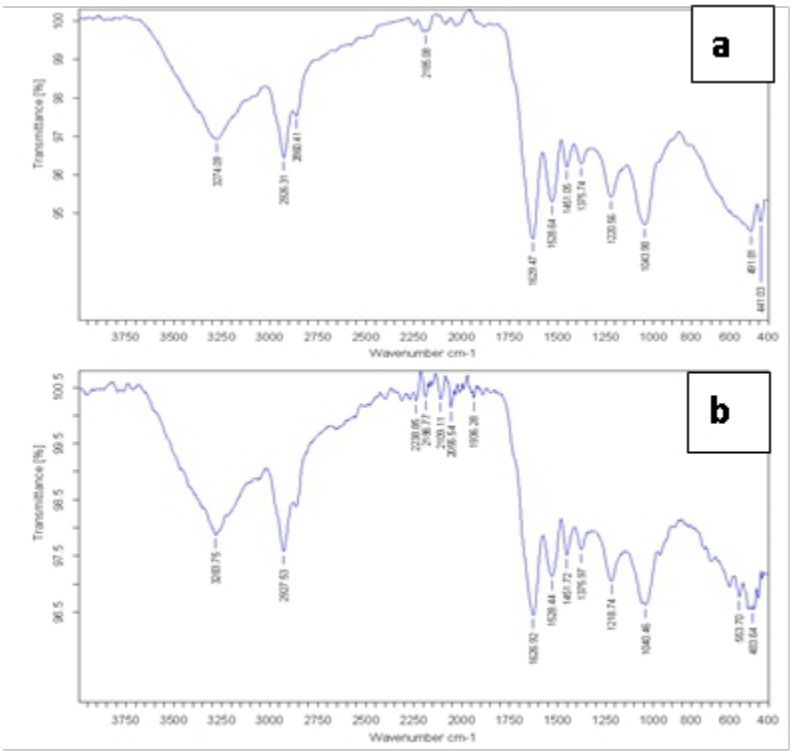


**Figure 11:** infrared spectra of the gold of the Haouanite deposit (a and b) corresponding to the images of figure 10 b and c.

In addition, we performed ICP analysis of 37 samples of all types (tab. 1, in annex). The results for the main elements are shown in Table 2. We then proceeded to a statistical treatment of these results as well as to a principal component analysis (Tab. 3 and Figs 12 and 13). It appears that:

- all rocks analyzed have relatively high gold amounts;
- gold does not correlate with any element except antimony and lead with which it shows a positive correlation. Remember that, for Trépanier (2007), this type of mineralization is characterized by chlorite, sericite, ankerite-compatible "greenschist" facies with a brittle to ductile-brittle tectonic control, which corresponds to the mineralization of the Jbel Haouanite deposit.

**Table 3:** Correlation matrix of the main elements established from geochemical analyzes

| | As | B | Ba | Be | Bi | Co | Cr | Cu | Li | Mo | Nb | Ni | Pb | Sb | Se | Sn | Sr | Y | Zn | Au |
|---|---|---|---|---|---|---|---|---|---|---|---|---|---|---|---|---|---|---|---|---|
| As | 1 | | | | | | | | | | | | | | | | | | | |
| B | 0,040 | 1 | | | | | | | | | | | | | | | | | | |
| Ba | -0,119 | 0,447 | 1 | | | | | | | | | | | | | | | | | |
| Be | **0,541** | 0,097 | -0,057 | 1 | | | | | | | | | | | | | | | | |
| Bi | -0,006 | 0,108 | -0,117 | -0,019 | 1 | | | | | | | | | | | | | | | |
| Co | 0,114 | **0,796** | 0,422 | 0,158 | 0,050 | 1 | | | | | | | | | | | | | | |
| Cr | -0,151 | 0,024 | 0,197 | -0,335 | 0,059 | 0,051 | 1 | | | | | | | | | | | | | |
| Cu | **0,615** | -0,063 | 0,042 | 0,337 | -0,009 | 0,149 | 0,394 | 1 | | | | | | | | | | | | |
| Li | -0,274 | 0,029 | -0,275 | -0,107 | 0,190 | -0,021 | -0,188 | -0,356 | 1 | | | | | | | | | | | |
| Mo | **0,529** | -0,276 | -0,004 | 0,176 | -0,302 | -0,157 | 0,083 | **0,631** | -0,368 | 1 | | | | | | | | | | |
| Nb | -0,190 | **0,607** | 0,439 | 0,073 | -0,070 | 0,350 | -0,117 | -0,248 | 0,007 | -0,260 | 1 | | | | | | | | | |
| Ni | 0,099 | 0,180 | 0,119 | -0,040 | -0,019 | 0,203 | **0,696** | **0,542** | -0,054 | 0,190 | -0,007 | 1 | | | | | | | | |
| Pb | 0,167 | 0,107 | 0,057 | -0,019 | -0,157 | 0,060 | 0,042 | 0,101 | -0,113 | 0,268 | -0,089 | -0,009 | 1 | | | | | | | |
| Sb | 0,157 | 0,097 | 0,055 | -0,025 | -0,156 | 0,052 | 0,040 | 0,099 | -0,112 | 0,268 | -0,087 | -0,013 | **0,999** | 1 | | | | | | |
| Se | -0,154 | **0,556** | 0,407 | 0,297 | 0,030 | 0,201 | -0,108 | -0,272 | 0,067 | -0,356 | **0,662** | 0,076 | 0,115 | 0,110 | 1 | | | | | |
| Sn | -0,294 | **0,574** | 0,348 | 0,011 | -0,004 | 0,357 | 0,068 | -0,293 | 0,128 | -0,377 | **0,655** | 0,155 | 0,015 | 0,008 | **0,752** | 1 | | | | |
| Sr | 0,364 | -0,081 | 0,040 | 0,628 | 0,027 | -0,148 | -0,203 | 0,287 | 0,058 | 0,221 | -0,056 | 0,081 | -0,030 | -0,036 | 0,361 | 0,059 | 1 | | | |
| Y | 0,338 | 0,456 | **0,621** | 0,154 | -0,006 | 0,352 | 0,306 | **0,511** | -0,244 | 0,303 | 0,445 | 0,361 | -0,059 | -0,062 | 0,191 | 0,064 | 0,139 | 1 | | |
| Zn | **0,648** | 0,055 | 0,043 | **0,533** | -0,221 | 0,149 | 0,003 | **0,608** | -0,212 | 0,434 | 0,008 | 0,274 | -0,044 | -0,052 | -0,133 | -0,214 | 0,452 | 0,443 | 1 | |
| Au | 0,230 | -0,153 | 0,121 | 0,165 | -0,007 | -0,150 | -0,048 | 0,187 | 0,095 | 0,189 | -0,072 | -0,081 | 0,354 | 0,356 | -0,009 | -0,334 | 0,132 | 0,150 | 0,211 | 1 |

For the classification of the Jbel Haouanite deposit, we took into account the fact that:

- the country rocks have undergone some "alterations / modifications", including (i) metasomatous carbonation with the appearance of ankerite-dolomite-calcite, (ii) the sodium metasomatism marked by the appearance of muscovite or biotite and (iii) the silicification of the country rocks in the immediate vicinity of the veins.
- mineralizations are carried by tectonic structures but are not associated with a specific direction;

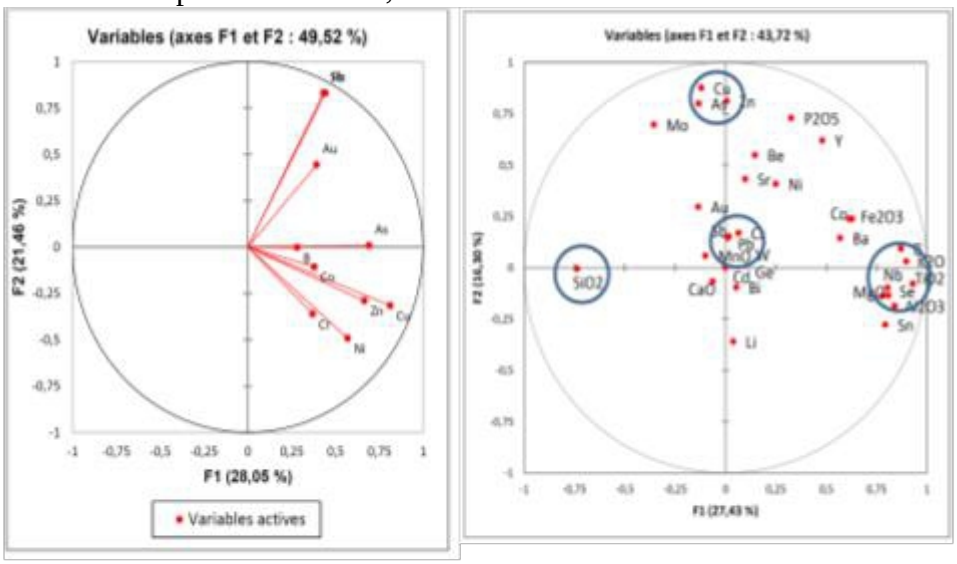


**Figure 13:** Diagram of the components 1 and 2 as a function of the weight of the metallic (a) and major and traces (b) elements in the rocks of the Haouanite deposit.

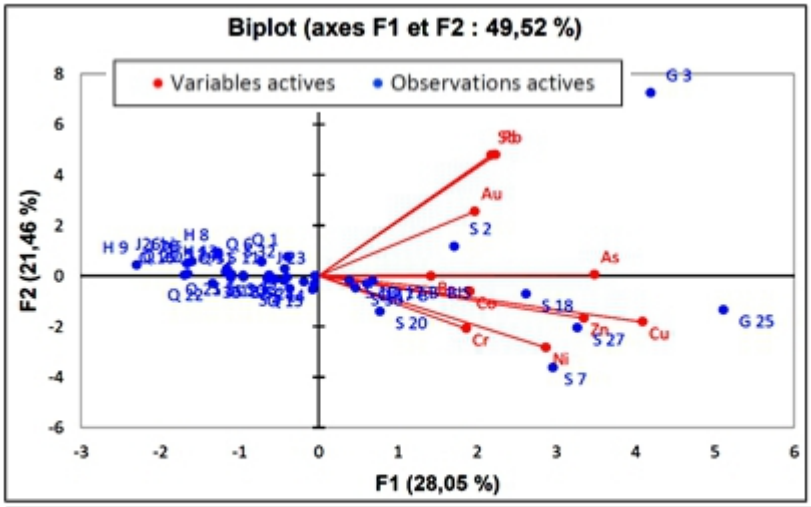


**Figure 12**: diagram of components 1 and 2 of the distribution of rocks according to the metallic elements (Au, Sb, pb, As, B, Co, Cu, Zn, Ni and Cr) composing the Haouanite deposit.

## Conclusion and genetic model

- The mineralization is not related to a given lithological facies;
- Gold is in free form in fractures or surrounded by a border of valentinite when it is associated with stibinite;
- Biotite and silicification are present in the host rocks in the immediate vicinity of the veins.

For the typology of the mineralizations, the results of the analyzes on the bi-logarithmic diagram of Poulsen et al. (2000), shows that the Jbel Haouanite mineralizations are essentially similar to the so-called "mesothermal" type, but also "epithermal" one (Fig. 14). This result allowed that the Jbel Haouanite deposit can be classified as mesothermal to epithermal orogenic deposits (Figure 15).

This study shows that the mineralizations are carried by quartz structures, generally E-W to NE-SW or NW-SE, and that the mineralized body is crushed and taken up by more or less flat late faults. Field and petrographic studies have shown that the formations have undergone at least three compressive phases inducing three phases of folding and three schistosities.

Similarly, although the region is known for the presence of several points of magmatic rocks, structural analysis made it possible to deduce that these magmatic intrusions are posterior to Visian but anterior to mineralization. A structural study made it possible to note thrusts of Ordovician quartzites on Silurian folded phtanites and the presence of thrust sheets affecting all formations.

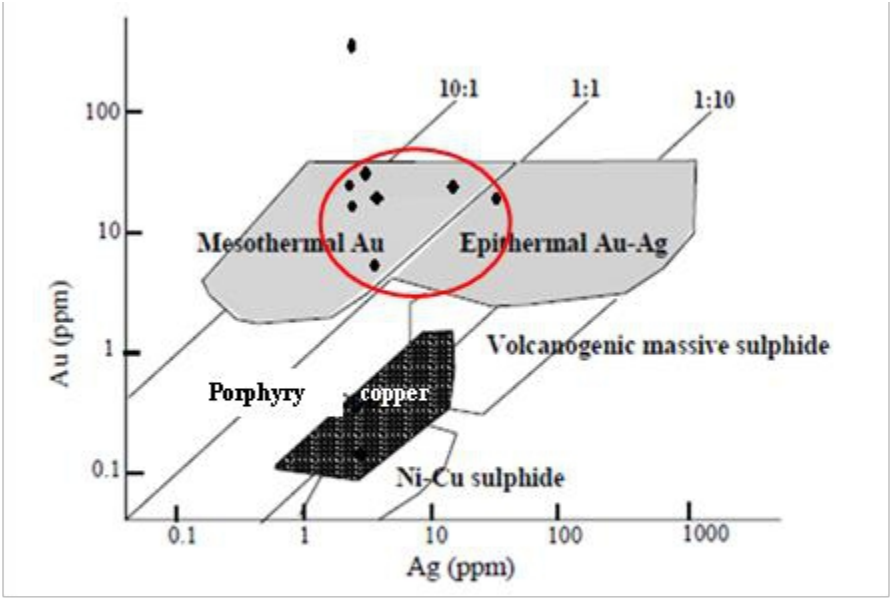


**Fig. 14 :** position des analyses de Jbel Haouanite sur le diagramme de Poulsen et al. (2000)

Metallographic studies have shown that the mineralization consists mainly of antimony sulfides and sulfosalts with free gold, which occurs in fissures of quartz veinlets or in areas of alteration of the stibnite where it is always surrounded by a border of valentinite.

Geochemical analyzes have shown, on the one hand, the abnormally high gold contents of all the rocks and, on the other hand, an independence of the gold which does not correlate with any element.

The analysis of the regional orogenic phenomena suggests that the mineralizations are finite to late-Hercynian. The engines will then look rather on the side of metamorphism and thrusts. Recall that for the mineralization of Menhouhou (south of the plain), Pelleter (2007) proposed an Ordovician age. But, as demonstrated in this study, most formations of Jbel Haouanite are post-Ordovician; so, there would have been several phases of remobilization before the current deposit.

Considering similar deposits, particularly those with gold and antimony from the Variscan chain of Western Europe, several similarities can be noted:

- mineralizations are carried by tectonic structures;
- the host rocks are essentially metamorphic;
- Gold is free or associated with sulphides or oxides (stibnite or valentinite);
- There is no direct link with magmatic intrusions.

The period of emplacement of the Au-Sb mineralization seems to be also similar within the different segments of the Variscan chain, whether in Morocco or in Europe. It seems to be synchronous with late-orogenic tectonic events resulting from a major tectonic regime change, namely the transition from a compressive regime to a dominant strike-slip regime (Arthaud and Matte 1977, Malavieille et al. 1990) and / or post-collapse extension of the chain (Bouchot et al., 2005).

**Acknowledgements**

The authors would like to thank all those who contributed to the realization and publication of this study, especially MM. Mouttaqi and Chaib of ONHYM for geochemical analyzes and M. Soulaimani (ENSMR, Rabat) for geostatistical treatment.

**References:**

1. Alansari A. (2008). *Rapport de la mission de prospection géologique effectuée dans le permis de la mine Ahad à Au-Sb.* Archives de la société Ahad, 44p, Inédit.
2. Arthaud F. & Matte P. (1977). *Late Paleozoic strike slip faulting in southern Europe and northern Africa: result of a right lateral shear zone between the Appalachians and the Urals*. Geol. Society of America Bulletin n° 88, pp. 1305-1320.
3. Azza A. & Makkoudi D (1996). *Cadre structural des minéralisations plombo-barytiques de Tafilalet.* Mines, Géol. Energie n° 55. pp. 175-184 ;
4. Bolata M. (1995). *Etude géologique de la région de Zelmou (Haut atlas oriental, Maroc)*. Thèse de doctorat, Univ. Mohammad V, Rabat, 173p.
5. Bouchot V., Ledru P., Lerouge C., Lescuyer JL. &Milesi JP. (2005). *Late Variscan mineralizing systems related to orogenic processes: The French Massif Central.* Ore GeolRev n°27, pp. 169-197.
6. Boutib L. (2000). *Etude géologique et structurale de la mine Ahad-Haouanite. Archives de la Société « Les Mines AHAD», 34p, Inédit,.*
7. Choubert G., Dresnay R. Du. &Hindermayer J. (1950). *Sur les calcaires à collenia de la région de Safsaf-AïnChaïr*. Notes du Serv. Géol. Maroc, t.3, n° 76, pp. 93-103.
8. Dresnay R Du & Lafuste J. (1960). *Lambeau du Dévonien à Aïn l'Orak dans le Nord du Tamlelt*. CR. Cong. Int. Stratigr. Silurien et Dévonien, Prague (1958) ; in Ust. Geol. Prague, pp. 452-453.
9. Dresnay R. Du &Wilfert S. (1960). *Présence de Skiddawien à graptolites dans le Haut Atlas oriental (Maroc)*. C. R. Acad. Sci. T : 250, n° 17, pp. 2915-2916.

10. El Kochri A. (1981). *Etude géologique de la boutonnière de Mougueur El Bour (Haut Atlas central)*. Thèse 3ème cycle, Univ. Paris VI,150p.
11. Groves D.I., Goldfarb R.J., Gebre-Mariam M, Hagemann SG & Robert F (1998). *Orogenic gold deposits—a proposed classification in the context of their crustal distribution and relationship to other gold deposit types*. Ore Geol. Rev. n° 13, pp. 7-27.
12. Hoepffner C. (1987). *La tectonique hercynienne dans l'Est du Maroc*. Thèse d'Etat, Univ Strasbourg, 280p.
13. Hoepffner C. ; Soulaimani A. & Piqué A. (2005). *The Moroccan hercynides*. Journal of African Earh Sciences, 43, pp. 144-165.
14. Houari M.R. (2003). *Etude de la boutonnière paléozoïque de Tamlelt (Haut Atlas oriental) : sa place dans la chaîne hercynienne du Maroc*. Thèse d'Etat, Fac. Sci. Oujda, 353 p.
15. Houari M.R. & Hoepffner C. (2000). *Structures des terrains paléozoïques à la limite sud de la chaîne hercynienne du Maroc (Haut Atlas Oriental)*. Africa Geoscience Review, Vol 7, N° 1, pp. 39-53.
16. Ingles J., Lamouroux C., Soula J-C., Guerrero N & Debat P. (1999). *Nucleation of ductile shear zones in granodiorite undergreenschist conditions, Néouvielle massif, Pyrenees, France*. Jour. Structural Geology n° 21, pp. 555-576.
17. Khoukhi Y. (2002). *Le paléozoïque inférieur du Haut Atlas Oriental (Maroc): dynamique sédimentaire, pétrologie et stratigraphie séquentielle.* Thèse, Univ. Mohamed Premier, Oujda
18. Malavieille, J., Guihot P., Costa, S., Lardeaux J.M. & Gardien V. (1990). *Collapse of the thickened crust in the French Massif Central: Mont Pilat extensional shear zone and St. Etienne Late Carboniferous basin.* Tectonophysics, n° 177, pp.139-149.
19. Milhi A., El Hmidi K., Benaissa H., Bouazza A., Raoufi M., Cheikh A., Chaieb M. & Barhdadi B. (2010). *Mémoire explicatif de la carte géologique du Maroc au 1/50 000 ; feuille de Jbel Lakhdar Ouest*. Notes et Mém. Serv. Géol ; Maroc, n° 449bis.
20. Pelleter E. (2007). *Géologie, géochimie et géochronologie du gisement aurifère de Tamlalt-Menhouhou (Haut Atlas oriental)*. Thèse INPL, Nancy, 237p.
21. Pelleter E., Cheilletz A., Gasquet D., Mouttaqi A., Annich M., El Hakour A. & Féraud G. (2008). *The Variscan Tamlalt-Menhouhou gold deposit, Eastern High-Atlas, Morocco*. Jour. African Earth Sci., N° 50, pp. 204-214.
22. Poulsen K.H., Robert F. & Dubé B. (2000). *Geological classification of Canadian gold deposits*. Geol. Surv. Canada, Bull. n° 540, 106 p.
23. Rey F. (1911). *Sur la présence du Gothlandien dans la plaine du Tamlelt (confins algéro-marocains)*. CRAS., T 152, n° 22, p 1532.

24. Trépanier S. (2007). *L'or dans les terrains de haut grade métamorphique*. Rap., Projet CONSOREM 2003-2A, Canada,74p.
25. Vasquez-Lopez R. (1974). *Présence d'or natif dans un filon de stibine du Jbel Haouanite*. Rap. SEGM, n° 954.

## Annex

**Table 1:** Nature and coordinates of the samples studied (Haouanite deposit)

| Sample | Nature | Coordinates | |
|---|---|---|---|
| | | X | Y |
| J23 | Siliceous rock of amorphous appearance | 02°27'13,9 | 32°34'20,6 |
| J26 | Jaspoïde | « « | « « |
| J 26bis | « « | « | « |
| S2 | Shale | « | « |
| S4 | Sandstone-like shale | 02°28'16 | 32°34'15,1 |
| S5 | | 02°28'16 ,7 | 32°34'10 |
| S7 | Satin shale, rich in white micas | 02°28'18,9 | 32°34'17 |
| S 10 | Satin shale | " | " |
| S 11 | Versicolored shade (Silurian?) | 02°28'29,2 | 32°34'31 |
| S12 | « « | "" | "" |
| S14 | « « | " | " |
| S 18 | Shale with ferruginous elements | 02°27'38,7 | 32°34'04,9 |
| S 19 | « « | 02°27'34,3 | 32°34'07,8 |
| S20 | Shale | 02°27'33,3 | 32°34'08,3 |
| S 24 | Mauve shale | 02°27'04,9 | 32°34'20 |
| S27 | « « | " | " |
| S 28 | « « | 02°27'04,8 | 32°34'09,4 |
| S30 | « « | « | « |
| S32 | « « | 02°27'43 | 32°34'15 |
| S33 | « « | 02°27'44,8 | 32°34'10,7 |
| S33 BIS | « « | « « | « « |
| G 3 | Mineralized body | 02°28'28,2 | 32°34'29,3 |
| G25 | Jaspe | 02°28'22,6 | 32°34'23 ,5 |
| H 8 | "granitoid", schistosed and fractured | 02°28'25 ?4 | 32°34'26 ,2 |
| H 9 | « | 02°2829,8 | 32°34'33,6 |
| H 13 | « | « | « |
| Q 1 | Quartz in veinlet (N 120 50SW) | 02°28'16,7 | 32°34'10 |
| Q 6 | Quartz | 02°28'07,3 | 32°34'44 ,1 |
| Q 15 | Folded quartz | « « | « « |
| Q 16 | Vein quartz | 02°28'07,6 | 32°34'11,9 |
| Q 17A | Quartzite | 02°27'33,8 | 32°34'10,6 |
| Q 21 | Pudding quartz | 02°27'21,8 | 32°34'19 |
| Q 22 | Quartz in millimetric veinlets | 02°27'26,4 | 32°34'08,5 |
| Q 29 | Quartz | 02°27'35,3 | 32°34'07,9 |
| Q 31 | Quartz | 02°28'07,7 | 32°34'11,9 |
| Q 17 B | « « | « « | « « |
| Q 17 B Bis | « « | 02°28'28,2 | 32°34'29,3 |

**Table 2:** Results of the analyses of the main chemical elements of the mining sector of Haouanite

| | Au | As | Sb | Pb | Zn | Cu | Co | Cr | Ni | B |
|---|---|---|---|---|---|---|---|---|---|---|
| **J 23** | 0,18 | 47 | 240 | 193 | 44 | 72 | 21 | 365 | 61 | 23 |
| **J 26** | 0,07 | 45 | 58 | 39 | 74 | 1 | 10 | 18 | 15 | 28 |
| **J26bis** | 0,09 | 43 | 57 | 38 | 75 | 1 | 10 | 19 | 15 | 29 |
| **S 2** | 0,3 | 129 | 1585 | 1570 | 116 | 47 | 80 | 128 | 73 | 115 |
| **S 4** | 0,03 | 25 | 102 | 44 | 48 | 111 | 57 | 149 | 57 | 67 |
| **S 5** | 0,03 | 32 | 45 | 39 | 56 | 23 | 58 | 37 | 59 | 99 |
| **S 7** | 0,03 | 6 | 65 | 82 | 98 | 164 | 61 | 681 | 536 | 85 |
| **S 10** | 0,03 | 59 | 69 | 53 | 68 | 46 | 59 | 50 | 52 | 98 |
| **S 11** | 0,06 | 25 | 79 | 72 | 86 | 1 | 86 | 83 | 38 | 124 |
| **S 12** | 0,03 | 58 | 35 | 94 | 151 | 44 | 49 | 26 | 29 | 50 |
| **S 14** | 0,03 | 52 | 67 | 57 | 112 | 30 | 104 | 54 | 60 | 126 |
| **S 18** | 0,09 | 212 | 169 | 266 | 146 | 149 | 101 | 73 | 125 | 145 |
| **S 19** | 0,11 | 69 | 229 | 185 | 347 | 2 | 25 | 152 | 33 | 83 |
| **S 20** | 0,03 | 25 | 42 | 45 | 65 | 156 | 72 | 531 | 53 | 73 |
| **S 24** | 0,03 | 26 | 66 | 52 | 29 | 1 | 65 | 57 | 27 | 128 |
| **S 27** | 0,03 | 156 | 73 | 106 | 411 | 264 | 43 | 109 | 181 | 35 |
| **S 28** | 0,03 | 75 | 82 | 60 | 110 | 28 | 71 | 69 | 55 | 117 |
| **S 30** | 0,03 | 93 | 78 | 62 | 70 | 95 | 101 | 72 | 64 | 105 |
| **S 32** | 0,13 | 15 | 88 | 65 | 63 | 20 | 79 | 84 | 54 | 118 |
| **S 33** | 0,05 | 87 | 69 | 81 | 95 | 22 | 61 | 100 | 42 | 72 |
| **33 BIS** | 0,03 | 85 | 71 | 79 | 97 | 21 | 63 | 103 | 46 | 73 |
| **G 3** | 0,2 | 119 | 27788 | 18358 | 66 | 100 | 61 | 151 | 56 | 85 |
| **G 25** | 0,19 | 295 | 196 | 274 | 476 | 259 | 66 | 133 | 139 | 46 |
| **H 8** | 0,19 | 16 | 59 | 90 | 79 | 20 | 18 | 24 | 15 | 19 |
| **H 9** | 0,03 | 13 | 69 | 51 | 21 | 3 | 5 | 13 | 15 | 20 |
| **H 13** | 0,03 | 125 | 66 | 56 | 40 | 21 | 23 | 29 | 15 | 19 |
| **Q 1** | 0,2 | 43 | 450 | 268 | 43 | 91 | 30 | 80 | 21 | 30 |
| **Q 6** | 0,16 | 32 | 30 | 31 | 50 | 10 | 68 | 57 | 47 | 63 |
| **Q 15** | 0,03 | 6 | 30 | 41 | 148 | 32 | 144 | 83 | 56 | 84 |
| **Q 16** | 0,03 | 20 | 30 | 27 | 39 | 26 | 23 | 124 | 25 | 12 |
| **Q 17 A** | 0,03 | 101 | 42 | 43 | 42 | 40 | 15 | 112 | 15 | 20 |
| **Q 21** | 0,03 | 62 | 30 | 24 | 43 | 49 | 28 | 132 | 23 | 29 |
| **Q 22** | 0,03 | 33 | 38 | 33 | 26 | 16 | 18 | 180 | 100 | 20 |
| **Q 29** | 0,03 | 33 | 30 | 31 | 16 | 28 | 25 | 125 | 20 | 19 |
| **Q 31** | 0,03 | 75 | 48 | 30 | 38 | 16 | 59 | 86 | 35 | 58 |
| **Q 17 B** | 0,09 | 109 | 372 | 118 | 132 | 147 | 36 | 70 | 70 | 21 |
| **Q 17 B-BIS** | 0,11 | 115 | 377 | 117 | 129 | 145 | 36 | 67 | 69 | 21 |

**Table 4:** analysis of major oxides (in %) and trace elements (in ppm) of magmatic rocks in the Jbel Haouanite sector

| Ech. | $SiO_2$ | $Al2O_3$ | CaO | $Fe_2O_3$ | $K_2O$ | MgO | MnO | $Na_2O$ | $P_2O_5$ | $TiO_2$ | P-Feu |
|---|---|---|---|---|---|---|---|---|---|---|---|
| **1** | 70,59 | 14,92 | 2,28 | 1,12 | 0,83 | 0,70 | 0,03 | 5,69 | 0,05 | 0,14 | 2,42 |
| **2** | 73,38 | 14,73 | 2,09 | 1,03 | 0,77 | 0,60 | 0,01 | 5,62 | 0,06 | 0,15 | 1,36 |
| **3** | 71,70 | 15,06 | 2,31 | 1,08 | 0,84 | 0,65 | 0,01 | 5,66 | 0,06 | 0,15 | 1,72 |
| **4A** | 73,17 | 14,60 | 2,18 | 1,10 | 0,88 | 0,58 | 0,01 | 5,96 | 0,06 | 0,14 | 1,35 |
| **4B** | 70,15 | 16,54 | 2,36 | 1,09 | 1,17 | 0,67 | 0,01 | 6,14 | 0,07 | 0,16 | 2,73 |
| **5** | 69,83 | 16,15 | 1,75 | 1,30 | 0,97 | 0,69 | 0,01 | 5,58 | 0,06 | 0,15 | 1,43 |
| **6** | 72,10 | 15,37 | 2,37 | 1,12 | 0,86 | 0,63 | 0,01 | 5,58 | 0,05 | 0,14 | 2,05 |
| **8** | 71,15 | 15,74 | 2,22 | 1,29 | 1,07 | 0,67 | 0,01 | 5,64 | 0,07 | 0,16 | 1,59 |
| **Ech.** | **Hg** | **Ba** | **Co** | **Cr** | **Ni** | **Sb** | **Sr** | **V** | **Y** | **Zr** | **Ta** |
| **1** | 104 | 299 | 6 | 38 | 8 | < 10 | 406 | 33 | < 5 | 36 | < 10 |
| **2** | < 10 | 304 | < 5 | 67 | 7 | < 10 | 415 | 31 | < 5 | 38 | < 10 |
| **3** | 43 | 304 | < 5 | 60 | 5 | < 10 | 463 | 29 | < 5 | 38 | 15 |
| **4A** | 10 | 295 | < 5 | 46 | 5 | < 10 | 431 | 27 | < 5 | 35 | < 10 |
| **4B** | 17 | 312 | < 5 | 60 | 7 | < 10 | 464 | 31 | < 5 | 36 | < 10 |
| **5** | 75 | 319 | 5 | 42 | 8 | < 10 | 355 | 38 | < 5 | 33 | < 10 |
| **6** | <10 | 346 | < 5 | 54 | 6 | < 10 | 462 | 34 | < 5 | 35 | < 10 |
| **8** | 10 | 295 | 5 | 57 | 7 | < 10 | 446 | 31 | < 5 | 38 | < 10 |